Journal of Applied Geophysics 119 (2015) 192–201

Contents lists available at ScienceDirect

Journal of Applied Geophysics

journal homepage: www.elsevier.com/locate/jappgeo

Separation of P–P and P–SV wavefields by high resolution parabolic Radon transform

Xiaoxue Jiang, Jun Lin, Fang Ye, Fan Zheng *

College of Instrumentation and Electrical Engineering, Jilin University, Changchun 130026, China

A R T I C L E I N F O

Article history:
Received 6 November 2014
Received in revised form 7 May 2015
Accepted 8 May 2015
Available online 15 May 2015

Keywords:
Three-component data
Wavefield separation
High resolution
Radon transform

A B S T R A C T

In three-component seismic reflection data, P–P and P–SV wavefield separation is an important issue which has great influence on interpretation and imaging. Under the assumption that P–P and P–SV wave reflections can approximately be regarded as parabolas when the offset is less than the depth, a P–P and P–SV wavefield separation method based on high resolution parabolic Radon transform is presented in this paper. By mapping three-component seismic data in the Radon model, P–P and P–SV waves separate from each other, after which separated wavefields are reconstructed by muting P–P and P–SV waves respectively in the transform domain. As the separation process relies on the focusing properties of both wave events in the Radon domain, the increased focusing power of the high resolution parabolic Radon transform enables separating P–P and P–SV wavefields robustly. Whereas the smearing problem of the conventional least squares parabolic Radon transform leads to poor separation suffering from residual energy, and the separating results by τ–p transform exhibits apparent amplitude distortion caused by event overlapping in the τ–p domain.

1. Introduction

The complete elastic wavefields recorded in three-component seismic data can provide more valuable insights than P-wave data alone (Baan, 2006). For example, P–P and P–SV wave data can obtain stack profiles respectively, and joint analysis of both wave data provides rich information on subsurface parameters such as anisotropy, lithology and porosity (Wang et al., 2002). It is often assumed in three-component seismics that the vertical z-component records are not only pure-mode P–P wave reflections but also contain P–SV converted wave energy. At the same time, the horizontal x-component contains both P–P and P–SV wave arrivals (Al-anboori et al., 2005). The contaminating energy on either component is unfavorable for seismic imaging and interpretation (Sun et al., 2004). Besides, successful P–P and P–SV wavefield separation improves the resulting depth images, reduces the overall noise level and facilitates sequence stratigraphic interpretation (Muijs et al., 2002).

P–P and P–SV wavefield separation may be performed in a number of different ways. Helbig and Mesdag (1982) presented a method to separate wavefields based on a motion product in the time-space domain. The wavefields are decomposed from the horizontal and vertical traces by using the signs of the motion products of P- and SV-waves. This method needs no true amplitudes, but is erroneous if P- and SV-arrivals are coincident at the receiver or if either the horizontal or vertical component is zero. Dankbaar (1985) developed a method of separating P- and S-waves that inverted the geophone records for the receiving characteristics using elastic wave equation and free surface condition. Devaney and Oristaglio (1986) described a method based on a plane-wave expansion to decompose P- and S-wave data, and introduced the equation for wavefield separation in the frequency domain. These wave equation based methods could obtain decent results when dealing with synthetic data, but due to the limited signal-to-noise ratio of real records and complex geological structures, their practical applications could not reach the expected effects, which include the attenuation of undesired wavefields and preservation of characters such as amplitude and waveform.

Several authors have applied the Radon transform to the wavefield separation problem. Tatham et al. (1983) and Tatham and Goolsbee (1984) separated P- and SV-wavefields by limiting the range in p-values during the $\tau - p$ transform for either the horizontal or vertical component and the separation was applied to offshore data. Greenhalgh et al. (1990) separated P- and SV-wavefields by forming a dot product between the signal vector and the slowness vector during projection of the seismic section into the $\tau - p$ space. Wang et al. (2002) proposed a $\tau - p$ domain scheme to separate P- and SV-wavefields by rotation of the horizontal and vertical components respectively. Al-anboori et al. (2005) developed a simplified version of the separation scheme of Greenhalgh et al. (1990), which has the advantage over exact wavefield separation schemes in that only a single parameter (the P-wave velocity for P–S wave enhancement or the S-wave velocity for P–P energy enhancement) needs to be specified. Liu et al. (2012) presented a method of separation of up-going and down-going waves from three-component crosswell seismic data using the $\tau - p$ transform. The above methods are all implemented by $\tau - p$ transform (i.e. linear Radon transform), and have achieved good performance. However, the

* Corresponding author.
E-mail address: zhengfan@jlu.edu.cn (F. Zheng).

http://dx.doi.org/10.1016/j.jappgeo.2015.05.011

$\tau - p$ transform is defined in terms of summation along linear paths, while P–P and P–SV waves are nonlinear events. Therefore, this transformation could not map P–P and P–SV wave data to "points", which results in P–P and P–SV wave energy overlapping in the $\tau - p$ domain, making it hard to separate directly.

In three-component seismic exploration, P–P and P–SV wave events can approximately be regarded as parabolas when the offset is less than the depth. We present the parabolic Radon transform instead of the $\tau - p$ transform to the wavefield separation problem. With the parabolic Radon transform projecting three-component seismic data to "points", P–P and P–SV waves separate from each other, after which we reconstruct separated wavefields by simply muting P–P and P–SV waves respectively in the transform domain. Furthermore, in order to make the separation more thoroughly, we apply a high resolution parabolic Radon transform to increase the focusing power by inhibiting the creation of smearing in the Radon panel. Synthetic data test is given to demonstrate the better performance of the high resolution parabolic Radon transform, compared with the $\tau - p$ transform, and the conventional least squares parabolic Radon transform. We end with a real data example.

2. Traveltime of P–P and P–SV waves

Fig. 1 is P–P and P–SV wave ray paths for a simple one-layer model. The P–P wave traveltime t_p is defined as (Yilmaz, 1987)

$$t_p = t_{p0}\sqrt{1+\frac{x^2}{4h^2}} \tag{1}$$

where x is the offset and h the depth. $t_{p0} = \frac{2h}{v_p}$ is the two-way zero offset traveltime and v_p is the velocity of the P–P wave.

When the offset x is less than the depth h, Eq. (1) can be expanded using Taylor series expansion as (Zhang, 2010)

$$t_p = t_{p0}\left\{1+\frac{1}{2}\left(\frac{x}{v_p t_{p0}}\right)^2-\frac{1}{8}\left(\frac{x}{v_p t_{p0}}\right)^4+\cdots\right\}. \tag{2}$$

Rounding off high order terms of Eq. (2), the P–P wave traveltime can be written as

$$t_p \approx t_{p0}+\frac{x^2}{2v_p^2 t_{p0}} \tag{3}$$

which describes a parabola in the time-offset domain.

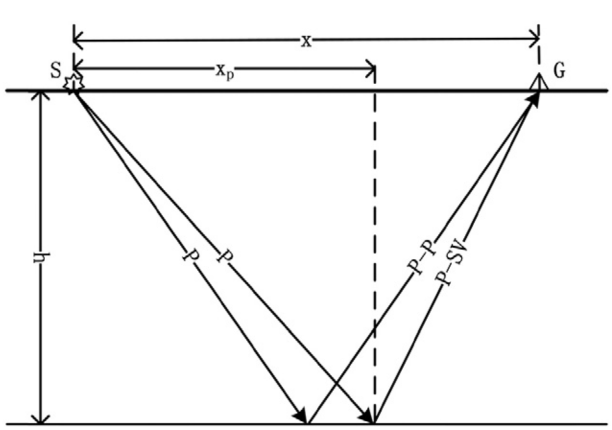

Fig. 1. P–P and P–SV wave ray paths for a simple one-layer model.

The P–SV wave traveltime t_s is defined as (Schneider, 2002)

$$t_s = \frac{\sqrt{x_p^2+h^2}}{v_p}+\frac{\sqrt{(x-x_p)^2+h^2}}{v_s} \tag{4}$$

where x_p is the horizontal coordinate of the conversion point and v_s the velocity of the P–SV wave.

Similar to P–P wave process, when the offset x is less than the depth h, expanding Eq. (4) using Taylor series expansion and rounding off high order terms, we obtain

$$t_s \approx \frac{h}{v_p}\left[1+\frac{1}{2}\left(\frac{x_p}{h}\right)^2\right]+\frac{h}{v_s}\left[1+\frac{1}{2}\left(\frac{x-x_p}{h}\right)^2\right]. \tag{5}$$

The horizontal coordinate of the conversion point x_p can be written as (Tessmer and Behle, 1988; Xu and Ma, 2002)

$$x_p \approx \frac{x}{1+\frac{v_s}{v_p}} \tag{6}$$

Using Eq. (6) to simplify Eq. (5), we obtain

$$t_s \approx t_{s0}+\frac{x^2}{2v_p v_s t_{s0}} \tag{7}$$

where $t_{s0} = \frac{h}{v_p}+\frac{h}{v_s}$ is the two-way vertical traveltime of the P–SV wave.

Eqs. (3) and (7) imply that P–P and P–SV wave events can both approximately be regarded as parabolas when the offset is less than the depth.

3. Linear Radon transform

The discrete forward $\tau - p$ transform from the time-offset domain to the intercept-slowness domain involves summation along linear trajectories (Schultz and Claerbout, 1978; Beylkin, 1987)

$$m(\tau, p_j) = \sum_{n=1}^{N} d(t = \tau + p_j x_n, x_n), j = 1, \ldots, M \tag{8}$$

where $d(t, x_n)$ denotes the seismic data and x_n the offset. $m(\tau, p_j)$ is the Radon panel, p_j the discrete slowness and τ the intercept time. N presents the number of seismic traces and M the number of slownesses.

Similarly, the conjugate transform (mapping from slowness space to offset space) involves summation along the slowness axis

$$d(t, x_n) = \sum_{j=1}^{M} m(\tau = t - p_j x_n, p_j), n = 1, \ldots, N. \tag{9}$$

Taking a temporal Fourier transform, the $\tau - p$ transform can be calculated for each temporal frequency ω

$$M(\omega, p_j) = \sum_{n=1}^{N} D(\omega, x_n) e^{i\omega p_j x_n}, j = 1, \ldots, M \tag{10}$$

$$D(\omega, x_n) = \sum_{j=1}^{M} M(\omega, p_j) e^{-i\omega p_j x_n}, n = 1, \ldots, N. \tag{11}$$

In matrix notation, Eqs. (10) and (11) can be written as

$$\mathbf{m} = \mathbf{L}^H \mathbf{d} \tag{12}$$

$$\mathbf{d} = \mathbf{L}\mathbf{m} \tag{13}$$